approximately 300 mμ long. Most of the remaining 10 percent are 200 mμ long, but a few shorter ones are still present.

The 200-mμ and shorter rods are removed by passing the concentrate through a 1 percent granulated agar-gel column 100-cm long and 1.5-cm in diameter (*8*). For this separation, the flow rate must be no greater than 5 ml per hour and the agar gel should be equilibrated with 0.01*M* EDTA, *p*H 7.5. The first fractions to contain virus, which can be detected by light scattering, consist almost entirely of standard-length (approximately 300 mμ) rods as determined by electron microscopy.

To obtain uniform suspensions of shorter rods, succeeding samples from the 1 percent agar-gel column are examined, and those containing a high percentage of the 200-mμ rods are collected, concentrated, and recycled through 1 percent agar-gel columns until the desired degree of uniformity is obtained. For uniform suspensions of still shorter rods, the supernatant liquids from the sedimentation for 20 minutes at 50,000*g* are centrifuged for 4 hours at 105,000*g*; the pellets are suspended in 0.001*M* EDTA, and the various fragments may be sorted on 5 percent granulated agar-gel columns equilibrated with 0.01*M* EDTA, *p*H 7.5. With these rod-shaped particles and the granulated agar-gel columns, there is no clear-cut separation into distinct fractions of rods of the different lengths, so some other method such as electron microscopy must be used to locate the position of desired lengths.

To avoid end-to-end aggregation after the particles are sorted by length, the ionic strength is decreased to 0.001*M* or less by concentrating the particles with high-speed centrifugation and resuspending them in 0.001*M* EDTA, *p*H 7.5, or by dialyzing the suspension against this same buffer.

Electron micrographs which illustrate the degree of homogeneity of fractions obtained by this procedure are shown on the cover of this issue. None of the sorted samples were truly monodisperse. They were obtained by only one or two passages through the appropriate agar-gel column, and the sorting under these conditions would probably require an additional passage or two to remove completely all particles of odd length from any fraction.

When opposite half leaves of susceptible hosts were inoculated with the various fractions, only standard-length (approximately 300 mμ) rods were infective, producing local lesions. No lesions were observed on half leaves inoculated with a suspension of the 200-mμ rods, the optical density of which equalled that of a standard preparation that produced over a hundred lesions on opposite half leaves. If the 200-mμ particles were capable of initiating infection on susceptible hosts, the fraction containing them should have given 50 percent more lesions than the standard preparation. No lesions resulted from inoculation of highly susceptible leaves with the still shorter fragments even at higher concentration. These results are in good agreement with those of Commoner *et al.* (*3*), who reported infectivity only for rods approximately 300 mμ long.

Since micrographs can be easily obtained which show uniform particle lengths, it is obvious that most of the shorter rods are not produced during the processes of preparing the suspensions for electron microscopy as postulated by Williams and Steere (*9*). Breakage of rods during preparation for electron microscopy appears to be restricted to those which overlap or lie across holes in the supporting film (*10*).

RUSSELL L. STEERE

Plant Virology Laboratory, Crops Research Division, U.S. Department of Agriculture, Beltsville, Maryland

References

1. W. M. Stanley, *Science* **81**, 644 (1935).
2. J. Symington, B. Commoner, M. Yamada, *Proc. Natl. Acad. Sci. U.S.* **48**, 1675 (1962).
3. B. Commoner, G. B. Shearer, M. Yamada, *ibid.*, p. 1788.
4. B. Commoner and J. Symington, *ibid.*, p. 1984.
5. H. Boedtker and N. S. Simmons, *J. Am. Chem. Soc.* **80**, 2550 (1958); B. S. Friesen and R. L. Sinsheimer, *J. Mol. Biol.* **1**, 321 (1959).
6. M. K. Corbett, *Virology* **15**, 8 (1961).
7. R. L. Steere and G. K. Ackers, *Nature* **194**, 114 (1962).
8. ———, *ibid.* **196**, 475 (1962).
9. R. C. Williams and R. L. Steere, *J. Am. Chem. Soc.* **73**, 2057 (1951).
10. I thank R. M. Faust for excellent technical assistance.

7 May 1963

Equilibrium Sedimentation of Uniform Rods of Tobacco Mosaic Virus

Abstract. *Equilibrium was achieved in centrifugal fields with tobacco mosaic virus by the Beams magnetically suspended ultracentrifuge. An attempt was made to account for the earth's gravitational component by using tilted cells in the rotor. The determinations of particle weight on highly uniform rods of tobacco mosaic virus in the apparent absence of nonideal behavior gave a value of (41.6 ± 0.1) 10^6.*

The equation for equilibrium in a centrifugal field relating distribution of solute to its molecular weight (*M*) is

$$M = \frac{2RT \ln (f_2c_2/f_1c_1)}{(1 - \bar{v}\rho)\, 4\pi^2N^2\, (x_2^2 - x_1^2)}$$

where c is the concentration of solute at any distance x from the axis of rotation, f is the activity coefficient, N is the frequency in revolutions per second, $\bar{v}$ is the partial specific volume of solute, ρ is the density of the solution and RT has its usual significance (*1*). The method offers a thermodynamic foundation for the study of the behavior of solutions in a multiphase system. Its usefulness for accurate data, however, has been limited to solutes substantially smaller than $M = 1 \times 10^6$ because of the uncertainty in N, convective disturbances, and the long time necessary to establish equilibrium at the low speeds required for larger solutes.

The Beams magnetically supported ultracentrifuge has overcome the above difficulties because the rotor, when suspended magnetically and coasting freely in a vacuum (10^{-6} to 10^{-7} mm-Hg), is inherently stable and free from hunting or precession at any angular velocity (*2*). Further, the optical system permits a precise knowledge of N and of the solute distribution at all points in the solution. The stability at low speeds also has made possible the application of the speed cutback procedure of Hexner *et al.* (*3*) to reduce the time required for reaching equilibrium by about one order of magnitude. The cutback method loses its advantage at low speeds unless all disturbances are avoided (*4*). Thus, one can use relatively long columns of solution ($\geqq$ 3 mm) to minimize uncertainties in the optical assessment of c as a function of x. Equilibrium with small polyhedral viruses ($M \cong 5 \times 10^6$) has been attained by these techniques (*5*). We have extended the centrifugal method for the study of particles larger by one order of magnitude. For this purpose tobacco mosaic virus (TMV) was chosen as solute. This order of size represents nearly the practical upper

limit for equilibrium in a centrifugal field; particles much larger than this virus ($M > 10^8$) may be studied with the earth's gravitational field alone (*6*).

Molecular-weight values reported for TMV vary greatly, although in recent years closer agreement has been achieved with different methods (*7*). The lack of a uniform value, however, may not be entirely a result of the measuring techniques. Separation of rods, both shorter and longer than the standard 3000-Å rod, in purified preparation, has proved difficult. In this study standard-size rods were separated from others on agar gel columns (*8*). After this purification, the rods were dialyzed against 0.01*M* sodium ethylenedinitrilotetraacetate (EDTA) buffer, *p*H 7.6, for the equilibrium runs. This medium, while not ideal, inhibits aggregation at low virus concentrations (*9*). Velocity sedimentation of these rods in a double-sector cell showed a clean single boundary which at 0.10 percent concentration of virus repeatedly yielded an s_{20} value of 180 ± 1*S*. The concentration was estimated from refractive measurements at 546 mμ. On the basis of dry-weight determinations the specific refractive increment in either water or in the EDTA medium at 20°C was 0.1853 ± 0.0004 ml/g. The value, 0.738 ml/g, which holds for concentrations up to 1 percent in the EDTA medium at 25°C (*9*), was used for the partial specific volume of the virus. The densities of the solutions used in the ultracentrifuge were taken from the density-concentration curve of Clarke *et al.* (*9*).

At rotor speeds above 10 rev/sec, the virus begins to sediment out of solution at a radius of 6.5 cm. Accordingly, the initial speed used to hasten equilibrium could not exceed this value, and the final speed had to be substantially less. Since the force at 10 rev/sec is already only about 26 times that of the earth's field, any reduction of speed markedly increases the effect of this vertical component on the sedimentation in the centrifugal direction. Thus, in radially aligned cells the interference fringes will not represent the passage of light through planes of uniform concentration. Maintaining a speed of 10 rev/sec, however, would require about 25 days to reach equilibrium with a 3-mm solution column. In order to utilize the cutback method, the centrifuge cell and the optics were tilted as diagrammed in Fig. 1. The angle, φ, at which the optical faces of the cell are tilted from the horizontal is given as

$$\varphi = \arctan [g(\omega_f^2 \cdot 6.5)^{-1}]$$

where g is 980.67 cm/sec^2 and ω_f, the final angular velocity, is $2\pi N$. The experiments were carried out at two final speeds between 5 and 8 rev/sec at the required angles of tilt from 8°00′ to 3°26′, respectively. Equilibrium was achieved with 3-mm columns throughout this speed range, although the upper speed was, experimentally, more ideal.

With radially aligned cells the molecular-weight equation in which interference fringes are used to assess the change in c with x is

$$M_w = \frac{RT\,(\lambda/k\alpha)\,(\Delta m)}{(1-\bar{v}\rho)\,\omega_f^2\,(x_2^2 - x_1^2)\,c_0}$$

where M_w is the weight-average molecular weight, λ is the wavelength of light (5461 Å), k is the specific refractive increment of virus in milliliters per 0.01 g, α is the depth of the column of solution in the direction of the light path (1.02 cm), Δm is the number of both constructive and destructive fringes in a radial direction through the column, and c_0 is the initial concentration of solute in grams per 100 ml. Modification of this equation to account for the gravitational effect is

$$M_w = \frac{RT\,(\lambda/k\alpha)\,\cos\varphi\,\Delta m}{(1-\bar{v}\rho)\,\omega_f^2\,(b^2\cos\varphi + 2r_0 b)\,c_0}$$

where b is the length of the solution column in the direction of sedimentation and r_0 is the distance from the axis to the meniscus at $\alpha/2$.

The results from several runs at different final speeds and concentrations in both tilted and untilted cells are given in Table 1. The data from experiments A, B, C, and D when plotted as the logarithm of concentration against the square of the radius were linear, indicating neither polydispersity (upward curvature) nor nonideality (downward curvature). Experiments A and B were conducted in a tilted cell and a graph of ln c against x^2 for A appears in Fig. 2*a*. Experiments C and D were performed with the conventional untilted cell, and a graph for D is shown in Fig. 2*b*. At these low concentrations no substantial discrepancy in the tilted-cell data was apparent. In experiments E, F, and G the solutions were not ideal throughout the cell. Figure 2*c* is a graph of experiment E where

Table 1. Molecular weight of tobacco mosaic virus by equilibrium sedimentation at 20.00°C.

Expt.	c_0 (g/100 ml)	N_f* (rev/sec)	Δm	φ	M_w (× 10^6)
A	0.096	6.185	12.64	3°26′	41.6
B	0.103	7.010	12.20	3°26′	41.5
C	0.091	6.420	9.76	0°00′	41.5
D	0.141	5.380	9.62	0°00′	41.7
E	0.360	6.500	32.60	0°00′	35.9
F	0.360	5.567	25.68	8°00′	38.5
G	0.160	8.080	22.88	3°26′	37.7

* In these experiments the initial speed was maintained at nearly 10 rev/sec for 47 hours before cutback to final speed (N_f). Usually the system was nearly at equilibrium shortly after cutback, but 1 to 2 days more were allowed to be certain of equilibrium.

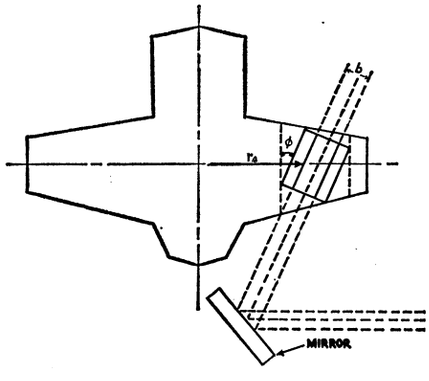

Fig. 1. Diagram of rotor with tilted cell.

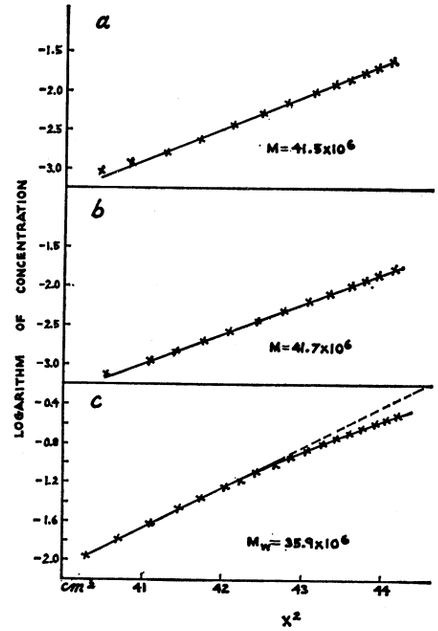

Fig. 2. Logarithm of c against x^2 from measurement of interference fringes at equilibrium: *a*, experiment A; *b*, experiment D; *c*, experiment E.

deviation from ideality became obvious at a virus concentration in the cell of about 0.3 percent and higher. Although the pattern of apparent deviation from ideality was similar in tilted and untilted cells, the fringe number at the equilibrium speed yielded a lower molecular weight with the untilted cell in the comparison runs E and F.

The molecular weights obtained in runs A and B (tilted cells) are probably quite close to the true particle weight of these rod samples. The modified equation, however, includes an approximation, due to the tilting which has, as an upper limit, an error of $\pm$ 1 percent. The uncertainty in the determination of c_0 is of this same order, while that from the determination of $\bar{v}$ is not yet well defined. The precision of the data from the magnetic ultracentrifuge for identical runs on small molecules is $\pm$ 0.5 percent. Assuming that the s_{20} value for these rods at 0.1 percent concentration is accurate, introduction of the mean molecular weight from experiments A through D (41.6×10^6) into the Svedberg equation yields a diffusion coefficient at this concentration of 0.403×10^{-7} cm^2/sec. This value is in good agreement with that determined on these same rods by free diffusion experiments (*10*).

From these preliminary studies it appears possible to define in a thermodynamically satisfactory manner the activity of large rods and to adduce shape information from a few experiments. For this purpose a more precise definition of components as well as other refinements may be desirable (*11*).

F. N. WEBER, JR., R. M. ELTON
H. G. KIM, R. D. ROSE
Department of Physics, University of Virginia, Charlottesville

R. L. STEERE
Plant Virology Laboratory, U.S. Department of Agriculture, Beltsville, Maryland

D. W. KUPKE
Department of Biochemistry, School of Medicine, University of Virginia

References and Notes

1. T. Svedberg and K. O. Pederson, *The Ultracentrifuge* (Oxford Univ. Press, New York, 1940), p. 51.
2. J. W. Beams, R. D. Boyle, P. E. Hexner, *Rev. Sci. Instr.* **32**, 645 (1961).
3. P. E. Hexner, L. E. Radford, J. W. Beams, *Proc. Natl. Acad. Sci. U.S.* **47**, 1848 (1961).
4. D. McIntyre, L. C. Williams, P. E. Hexner, H. G. Kim, F. N. Weber, Jr., R. F. Bunting, D. W. Kupke, *J. Polymer Sci.* **62**, S136 (1962); R. F. Bunting and P. E. Hexner, unpublished results.
5. P. E. Hexner, D. W. Kupke, H. G. Kim, F. N. Weber, Jr., R. F. Bunting, J. W. Beams, *J. Am. Chem. Soc.* **84**, 2457 (1962).
6. F. N. Weber, Jr., D. W. Kupke, J. W. Beams, *Science* **139**, 837 (1963).
7. H. Boedtker and N. S. Simmons, *J. Am. Chem. Soc.* **80**, 2550 (1958).
8. R. L. Steere, *Science*, this issue.
9. A. M. Clarke, D. W. Kupke, J. W. Beams, *J. Phys. Chem.* **67**, 929 (1963).
10. W. Möller, private communication.
11. Supported by grants GM-10860 and A-4005 from the U.S. Public Health Service. F.N.W. is a predoctoral fellow of the U.S. Public Health Service and H.G.K. is an American Machine and Foundry fellow. We are indebted to Professor J. W. Beams for ideas and advice and thank T. E. Dorrier and Katherine Whiting for special assistance.

13 May 1963

Molecular Model for Protein Synthesis

Abstract. *Molecular models constructed for RNA, adapter RNA, and the ribosome are consistent with available physical-chemical data. These components can be assembled to produce a stereochemically sound model for the template mechanism in protein synthesis.*

The arrangement of amino acids in proteins is one of nature's greatest complexities (*1*). Yet man has, within the short span of a decade, almost completely solved its mystery. The theory of how amino acids are ordered was proposed by Crick (*2*), and is shown in Fig. 1. Amino acids are linked to specific adapter-RNA molecules; these become transferred to the ribosome, where the adapter RNA's are joined by hydrogen bonds to complementary sites on an RNA template—called messenger RNA—and the amino acids are placed in the proper juxtaposition for peptide synthesis. The latter is a sequential process, proceeding from the N-terminal to the C-terminal amino acid (*3*).

A great deal is known about the molecular structures of adapter RNA, messenger RNA, and the ribosome. As a result it has been possible to consider more constructively the exact nature of the template mechanism for protein synthesis (*4*). First let us consider the molecular structure of adapter RNA.

The x-ray diffraction pattern of total adapter RNA bears a strong resemblance to the diffraction pattern given by DNA (*5*). The sharpness of the main equatorial reflection indicates a regularity in packing between molecules paralleled only by the best samples of DNA which have been studied. The orientation observed for the equatorial 23 Å and meridional 3.3 Å spacing strongly confirm this double-helical nature. It has been argued by Doty *et al.* (*6*) that hyperchromasy may be taken as evidence for the existence of a helical secondary structure for polynucleotides in solution. Such studies on adapter RNA suggest that it maintains its double-helical configuration in solution since on heating from room temperature in physiological saline, the optical density of adapter RNA rises gradually until there has been an increase of about 30 percent. A regular double helix of high molecular weight, like DNA, does not increase in optical density until a temperature of about 80°C is reached, at which point it increases abruptly by about 40 percent. The smaller and more gradual increase in hyperchromasy shown by adapter RNA might be caused by irregularities in the base pairing. Alternatively, it might be the result of its short double helix, which, even if perfectly regular, would include only about 30 base pairs.

Recently, Spencer and his co-workers (*7*) succeeded in crystallizing a soluble RNA fraction from yeast, which they believe to be the adapter RNA. The regularity of the x-ray diffraction patterns of such material has led them to propose that adapter RNA from yeast has completely regular Watson-Crick type base pairing. But small irregularities in base pairing would be very difficult to detect from such preliminary observations, and we believe that the exact nature of adapter RNA base pairing is still uncertain.

In solution, the molecular weight of adapter RNA determined by ultracen-

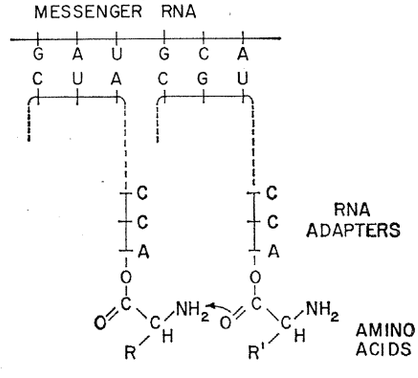

Fig. 1. The function of adapter RNA in protein synthesis. Amino acids are linked to specific adapter RNA's. These become transferred to the ribosome, where the adapter RNA's form hydrogen bonds at complementary sites on the template, placing the amino acids in the proper juxtaposition for peptide synthesis.